Tanshinone IIA regulates expression of glucose transporter 1 via activation of the HIF-1α signaling pathway

YANYUN ZHOU[1,2*], HONG ZHANG[2*], YITONG HUANG[1], SHENGYUN WU[1] and ZONGJUN LIU[2]

[1]Central Laboratory and [2]Department of Cardiovascular Medicine, Putuo Hospital, Shanghai University of Traditional Chinese Medicine, Shanghai 200062, P.R. China

Received May 5, 2022; Accepted July 29, 2022

DOI: 10.3892/mmr.2022.12844

Abstract. Tanshinone IIA (Tan 2A) is a lipid-soluble compound extracted from the Chinese herb Danshen (*Salvia miltiorrhiza Bunge*). It protects neuron and microvascular endothelial cells against hypoxia/ischemia both *in vitro* and *in vivo* however the mechanism is not fully known. Glucose transporter 1 (GLUT-1) is ubiquitously expressed in all types of tissue in the human body and serves important physiological functions due to its glucose uptake ability. The present study evaluated the role of Tan 2A in regulating GLUT-1 expression and its potential mechanism. RT-PCR and western Blot were used to detect the expression of GLUT-1. Si RNA mediated knockdown and CHIP assay were used to explore the mechanism of Tan 2A on GLUT-1expression. Tan 2A treatment induced expression of GLUT-1 and subsequently increased glucose uptake in endothelial cells (ECs). Furthermore, mRNA expression levels of vascular endothelial cell growth factor, BCL2 interacting protein 3 and enolase 2, which are target genes for hypoxia-inducible factor-1α (HIF-1α), were significantly upregulated by Tan 2A. Co-immunoprecipitation demonstrated that Tan 2A markedly increased the association of HIF-1α with recombination signal-binding protein for immunoglobulin κJ region (RBPJκ). Moreover, knockdown of HIF-1α and RBPJκ significantly reversed the regulatory effect of Tan 2A on mRNA expression levels of these genes in ECs. The results of the present study suggested that HIF-1α partially mediated the regulatory effect of Tan 2A on GLUT-1 expression in ECs. Therefore, GLUT-1 may be a potential therapeutic target for Tan 2A.

Correspondence to: Dr Zongjun Liu, Department of Cardiovascular Medicine, Putuo Hospital, Shanghai University of Traditional Chinese Medicine, 164 Lanxi Road, Putuo, Shanghai 200062, P.R. China
E-mail: liuzongjun1548@shutcm.edu.cn

*Contributed equally

Key words: Tanshinone IIA, human umbilical vein endothelial cell, glucose transporter-1, hypoxia-inducible factor-1α, recombination signal-binding protein for immunoglobulin κJ region

Introduction

The brain utilizes high levels of energy to maintain its physiological function. The mammalian brain depends on glucose as its main source of energy but lacks oxygen and glucose reserves and therefore requires a continuous supply of glucose from blood (1). Two independent groups of transporter proteins, glucose transporters (GLUTs) and solute carrier family members, mediate glucose transport into the brain (2). GLUT protein 1 (GLUT-1), also called solute carrier family 2 member 1, was first identified in a fetal skeletal muscle cell line (3) and is ubiquitously expressed in all types of tissue (4). It is also reported to be highly expressed in endothelial cells (ECs) of the central nervous system and is considered to be the principal glucose transporter of the blood-brain barrier (5). Functional deficiency of GLUT-1 decreases the amount of glucose available to brain cells, which affects brain function (6).

Danshen (*Salvia miltiorrhiza Bunge*), a medicinal herb, has been used in traditional Chinese medicine to treat conditions associated with the cardiovascular and cerebrovascular systems, such as stroke (7). Tanshinones are the primary active component of Danshen. Tanshinone IIA (Tan 2A), the most abundant diterpenoid quinone in *S. miltiorrhiza*, a natural inhibitor of monoacylglycerol lipase, is a fat-soluble component and is reported to exert anti-inflammation, anti-cancer, neuroprotection and hypolipidemic activity (8,9), and have a neuroprotective and cardiovascular protective effect. Tan 2A increases blood flow in the heart and improves myocardial metabolic disorder by increasing the tolerance of cardiomyocytes to hypoxia (10). Tan 2A protects neuron and microvascular ECs against hypoxia/ischemia both *in vitro* and *in vivo* (11). Tan 2A sodium sulfonate decreases atherosclerotic lesion area by inhibiting expression of intracellular chloride channel 1 in ECs (12) and activating Kruppel-like factor 4 in macrophages (13,14). The combination of Danshen and Sanqi (a Chinese herbal medicine) prescription has been reported to markedly increase expression of liver glycogen synthesis genes, such as GLUT-1, and improve fat and glucose metabolism (15). To the best of our knowledge, however, whether GLUT-1 expression of ECs is regulated by Tan 2A is not yet known. It was hypothesized that Tan 2A may induce glucose uptake via regulation of GLUT1 expression in vascular ECs.

Previous studies have reported that hypoxia-inducible factor 1 α (HIF-1α) may mediate the therapeutic actions of Tan 2A (16,17). For example, Tan 2A is reported to inhibit breast cancer growth by inhibiting HIF-1α expression via the mammalian target of rapamycin signaling pathway (18). Tan 2A also blocks epithelial-mesenchymal transition in breast cancer cell lines by regulating the HIF-1α signaling pathway (19). Tan 2A decreases the inflammatory response in LPS-induced lung injury via the HIF-1α signaling pathway (20). Furthermore, overexpression of GLUT-1 enhances the effect of Tan 2A on the treatment of middle cerebral artery occlusion (21). The present study assessed the regulatory effect of Tan 2A on expression of GLUT-1 in ECs and evaluated whether the effect of Tan 2A was associated with HIF-1α.

Materials and methods

Cell culture and reagents. Human umbilical vein endothelial cells (HUVECs) were purchased from ScienCell Research Laboratories, Inc. and cultured in EC medium containing EC growth supplement (ScienCell Research Laboratories, Inc.), 5% fetal bovine serum (FBS; ScienCell Research Laboratories, Inc.), 100 U/ml penicillin and 100 U/ml streptomycin in 37˚C. HUVECs at passages 3-5 were used for all experiments. Tan 2A was purchased from Selleck Chemicals (Cat. no. S2365, Lot no. S2767130005001). DMSO (sigma-Aldrich; Merck KGaA) was used as vehicle control. Lipofectamine™ RNAiMAX Transfection Reagent and Lipofectamine® 3000 Transfection Reagent were purchased from Invitrogen (Thermo Fisher Scientific, Inc.). Antibody against GLUT-1 (ab115730, 1:2,000) was purchased from Abcam. Antibodies against HIF-1α (#36169, 1:1,000), RBPJκ (#5313, 1:1,000) and GAPDH (#5174, 1:2,000) and horseradish peroxidase-conjugated goat anti-rabbit (#7074, 1:2,000) or anti-mouse secondary antibodies (#7076, 1:2,000) were purchased from Cell Signaling Technology, Inc.

Transfection and gene silencing. Small interfering (si)RNAs targeting human GLUT-1, HIF-1α and recombination signal-binding protein for immunoglobulin κ J region (RBPJκ) were synthesized by Shanghai GenePharma Co., Ltd. siRNA (100 nM) were transfected into cells using Lipofectamine RNAiMAX Transfection Reagent in room temperature for 10 min. About 48 h later, the cells were extracted for RNA or protein detection. Scrambled siRNA was used as a negative control (Shanghai GenePharma Co., Ltd.). siRNA sequences are presented in Table SI.

Reverse transcription-quantitative (RT-q)PCR. Total cellular RNA was extracted using RNAiso Plus (Code No.: 9109, Takara Biotechnology Co., Ltd.). Complementary (c)DNA was synthesized from total RNA using PrimeScript RT reagent Kit with gDNA Eraser (Takara Biotechnology Co., Ltd. TKR-RR047) as follows: 42˚C for 2 min, 37˚C for 15 min and then 85˚C for 5 sec. Primer sequences are presented in Table SI. qPCR was performed using SYBR-Green Master Mix (Takara Biotechnology Co., Ltd.). The thermocycling conditions were as follows: Pre-denaturation at 94˚C for 5 sec; followed by 40 cycles of denaturation, 95˚C for 5 sec, annealing at 60˚C and extension for 34 sec. The 18s rRNA was used as an internal control (Sangon Biotech Co., Ltd.). The mRNA expression level of each target gene was determined using the $2^{-\Delta\Delta Cq}$ method (22).

Plasmid and luciferase activity assay. The DNA fragment containing the hypoxia-responsive element (HRE) sequence (TGTCACGTCCTGCACGACTCTAGT) was subcloned into the pGL3 basic reporter vector (Promega Corporation). The plasmid luciferase reporters were electroporated into HUVECs using an ECM 839 Electroporation System (Harvard Apparatus) as previously reported (23). Briefly, HUVECs were resuspended in EC medium (without serum; ScienCell Research Laboratories, Inc.), 20 μg plasmid was added and mixed in MicroPulse Cuvettes (0.4 cm, Bio-Rad). The cuvettes are one-piece injection molded chambers with embedded aluminum electrodes and square sealing caps. An electrical pulse (160 mA, 1 ms, 1 pulse) was applied. Cells ($2x10^4$) were then seeded in 24 wells plates immediately using EC medium at room temperature for 24 h. The transactivation activity was analyzed using the Dual-Luciferase Reporter Assay System (Promega Corporation) according to the manufacturer's instructions. Briefly, 1X Passive Lysis Buffer was dispensed into each culture vessel for 15 min at room temperature. Then the cell lysis was mixed with Luciferase Assay Substrate and measured firefly luciferase activity in GloMax 20/20 Luminometer (Promega).

Western blotting. HUVECs were lysed with RIPA buffer (Thermo Fisher Scientific, Inc.) with protease inhibitors (Cell Signaling Technology, Inc.). The protein concentration was determined using the bicinchoninic acid protein assay (Thermo Fisher Scientific, Inc.). A total of 20 μg/lane protein sample was resolved on 10% SDS-PAGE and electrotransferred to polyvinylidene fluoride membranes. The immunoblots were blocked with 5% BSA (Sangon Biotech Co., Ltd) for 1 h at room temperature, and probed with the aforementioned antibodies overnight at 4˚C, followed by incubation with the corresponding secondary antibodies for 1 h at room temperature. Subsequently, the membranes were washed with TBS-Tween (0.1%) three times, 10 min each. The blots were visualized using Clarity Western ECL Substrate (Bio-Rad Laboratories, Inc.). GAPDH was used as an internal reference. Densitometry analysis was performed using ImageJ (V1.8.0.112; National Institutes of Health).

Glucose uptake assay. Glucose uptake assay was performed using the Colorimetric Glucose Uptake Assay kit (Abcam) according to the manufacturer's protocol. Briefly, 2-deoxyglucose (2-DG) was added to HUVECs and incubated for 20 min at 37˚C. After 2-DG was taken up by glucose transporters and metabolized to 2-DG-6-phosphate, the cells were washed with phosphate-buffered saline (PBS) to remove exogenous 2-DG. Cells were lysed using repeated pipetting, freeze/thaw and heating at 85˚C for 40 min. The level of 2-DG-6-phosphate in each sample was determined by enzymatic recycling amplification reaction and analyzed using a microplate reader (optical density, 412 nm) in kinetic mode at 37˚C.

Co-immunoprecipitation (Co-IP) assay. HUVEC protein was collected using Pierce™ IP lysis buffer (Thermo Fisher

Scientific, Inc.) and centrifugation at 12,000 g, 4˚C for 10 min, supernatant including protein were collected. Protein lysate (400 μg) was immunoprecipitated with the RBPJκ antibody (2 μg/well; CST, Inc.; cat. no. #5313) or control Rabbit IgG control Polyclonal antibody (2 μg/well; ProteinTech Group, Inc.; cat. no. 30,000-0-AP) bound to Dynabeads Protein G (50 μl/tube) by using Immunoprecipitation Kit-Dynabeads Protein G (Thermo Fisher Scientific, Inc.) according to manufacturer's instructions. Completes were isolated by addition of 20 μl IP lysis buffer (Thermo Fisher Scientific, Inc.) and 5 μl SDS-PAGE SDS Sample Loading Buffer (5X, Beyotime, cat. no. P0015L) and heat for 5 min at 100˚C, then place the tube on the DynaMag-Spin (Thermo Fisher, cat. 12320D) and load the supernatant/sample onto a gel and assessed using western blotting as per the aforementioned method.

Chromatin IP (ChIP) assay. ChIP assay was performed according to the manufacturer's instructions using Magna ChIP G-Chromatin Immunoprecipitation kit; cat. no. 17-611; Millipore). Briefly, HUVECs were treated with Tan 2A (20 μM) for 16 h in 37˚C. 275 μl 37% formaldehyde (Sangon Biotech Co., Ltd.) was added to 10 ml of growth media to cross-link protein to chromatin for 10 min at room temperature, then quenched with glycine at a final concentration of 125 mM immediately at room temperature for 5 min. Cells were harvested in cold PBS. The cellular nuclear pellets were resuspended with sonication buffer. The resulting cell suspension was sheared by sonication (MiSonix Sonicator 3000) on ice using 30/30-sec on/off for 10 min (Output Power: 4). ChIP assay was performed using 1.5 μg Rabbit IgG (1.15 mg/ml, ProteinTech Group, 30000-0-AP) or anti-HIF-1α antibodies (CST, #14179) bounded to the Magnetic Protein G beads. Each IP requires the addition of 500 μl Dilution Buffer. Wash the Protein G bead-antibody/chromatin complex by resuspending beads in 0.5 ml each of the cold buffers in the order listed below [Low Salt Immune Complex Wash Buffer (cat.# 20-1 54), High Salt Immune Complex Wash Buffer (cat.# 20-1 55), High Salt Immune Complex Wash Buffer (cat.# 20-1 55), High Salt Immune Complex Wash Buffer (cat.# 20-1 55)]. The DNA fragment containing the HRE site was amplified by qPCR (SYBR-Green Master Mix, Takara Biotechnology Co., Ltd.) using the following primers: forward: 5'-TGGGAAAAG GCATAGACTGG-3', reverse: 5'-ATGCACGAATGAGTG AGCAG-3') specific for the HRE site were synthesized for this purpose. Reference gene primer sequences are as follows: forward: 5'-GTAACCCGTTGAACCCCATT-3', reverse: 5'-CCATCCAATCGGTAGTAGCG-3'. PCR conditions were Pre-denaturation, 94˚C for 5 sec; followed by 40 cycles of denaturation, 95˚C for 5 sec, annealing at 60˚C and extension for 34 sec. The DNA expression level of each target gene was determined using the 2-ΔΔCq method (22).

RNA sequencing (RNAseq). Total RNA was extracted using mirVana miRNA Isolation Kit (Ambion) following the manufacturer's protocol. RNA purity and quantification were evaluated using a NanoDrop 2000 spectrophotometer (Thermo Fisher Scientific, Inc.). RNA integrity was assessed using an Agilent 2100 Bioanalyzer (Agilent Technologies, Inc.). Libraries were constructed. The transcriptome sequencing and analysis were performed by OE Biotech Co. Ltd. The libraries were constructed using TruSeq Stranded mRNA LTSample Prep Kit (RS-122-2101/RS-122-2102/RS-122-2103, Illumina, Inc.) according to the manufacturer's instructions. A total of 10 pM loading concentration was used. Sequencing kits were as follows: NovaSeq 6000 S4 Reagent Kit V1.5 (300 cycles; Illumina, Inc., Catalog no. 20028312) and NovaSeq Xp 4-Lane kit v1.5 (Illumina, Inc., cat. no. 20043131). The libraries were sequenced on the Illumina sequencing platform (Illumina HiSeq X Ten) and 125 or 150 bp paired-end reads were generated. Fragments Per Kilobase of transcript per million fragments mapped value of each gene was calculated using cufflinks and read counts of each gene were obtained by HTSeqcount. Differential expression analysis was performed using the DESeq2 (1.20.0) R package. $P<0.05$ and fold-change >2 or <0.5 was set as the threshold for significantly different expression.

Bioinformatics. Hierarchical cluster analysis of differentially expressed genes was performed to explore genes expression pattern. Gene Ontology (GO, http://geneontology.org/) enrichment and Kyoto encyclopedia of genes and genome (KEGG, http://www.genome.jp/kegg/) pathway enrichment analysis of differentially expressed genes were performed using R (R-v3.4.2, r-project.org) based on the hypergeometric distribution. GO datasets used in this research were as follows: response to hypoxia (GO:0001666), regulation of GPCR signaling (GO:0008277), protein homooligomerization (GO:0051260), brain development (GO:0007420), angiogenesis (GO:0001525), negative regulation of cell proliferation (GO:0008285), positive regulation of cell proliferation (GO:0008284), GPCR signaling (GO:0007186), transcription from RNA pol 2 promoter (GO:0045944), transcription, DNA-templated (GO:0006351).

Statistical analysis. The data are presented as the mean ± SEM. Each experiment was independently repeated three times. Statistical significance was calculated using one-way ANOVA and Tukey's multiple comparison test for ≥3 groups. Unpaired Student's t-test was used for comparison between two groups. $P<0.05$ was considered to indicate a statistically significant difference.

Results

Tan 2A increases GLUT-1 expression and glucose uptake in HUVECs. To assess the effect of Tan 2A on GLUT-1 expression, HUVECs, a commonly used model for ECs (24), were treated with Tan 2A at 0, 15 and 30 μM for 24 h and 15 μM for 24 and 36 h. RT-qPCR results demonstrated that mRNA expression levels of GLUT-1 in HUVECs exposed to 15 μM Tan 2A increased significantly at 24 and 36 h compared with 0 h control (Fig. 1A). The relative mRNA expression levels of GLUT-1 increased significantly to 3.18±0.32 and 3.65±0.51 following 15 and 30 μM treatment for 24 h, respectively, compared with the 0 h control. And (Fig. 1B). Furthermore, GLUT-1 protein expression levels were assessed using western blotting. The protein expression levels were consistent with the mRNA expression levels of GLUT-1, also exhibiting upregulation by Tan 2A (Fig. 1C and D). Moreover, endothelial glucose uptake was assessed using glucose

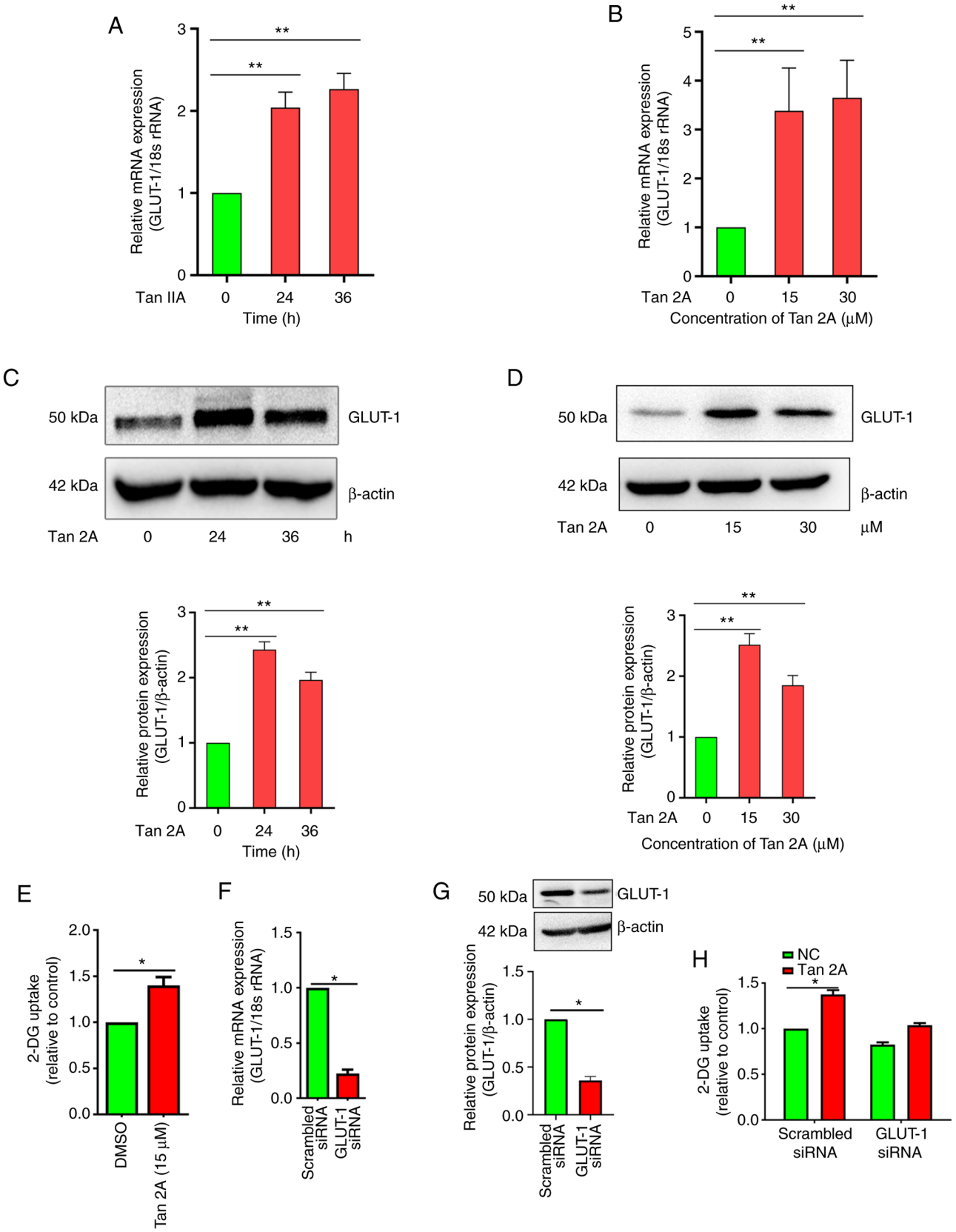

Figure 1. Tan 2A increases expression of GLUT-1 in HUVECs. (A) HUVECs were treated with Tan 2A or DMSO for 24 and 36 h and GLUT-1 relative mRNA expression levels were examined using RT-qPCR. (B) RT-qPCR of GLUT-1 relative mRNA expression levels in HUVECs treated with Tan 2A at 15 and 30 μM or DMSO for 24 h. ECs were treated with Tan 2A for (C) different durations or (D) increasing concentrations for 24 h and protein expression levels of GLUT-1 were assessed using western blotting. (E) Glucose uptake in HUVECs was assessed following treatment with Tan 2A for 24 h using Colorimetric Glucose Uptake Assay Kit. (F) HUVECs were transfected with siGLUT-1 or scrambled siRNA as a control for 48 h and (G) relative mRNA and protein expression levels of GLUT-1 were detected by RT-qPCR and western blotting, respectively. (H) HUVECs were transfected with siGLUT-1 or control siRNA for 24 h and treated with Tan 2A for 24 h. Data are presented as the mean fold increase ± SEM of three independent experiments. *P<0.05 and **P<0.01. Tan 2A, Tanshinone 2A; HUVEC, human umbilical vein endothelial cell; RT-q, reverse transcription-quantitative; GLUT-1, glucose transporter 1; 2-DG, 2-deoxy-glucose; si, small interfering; NC, negative control.

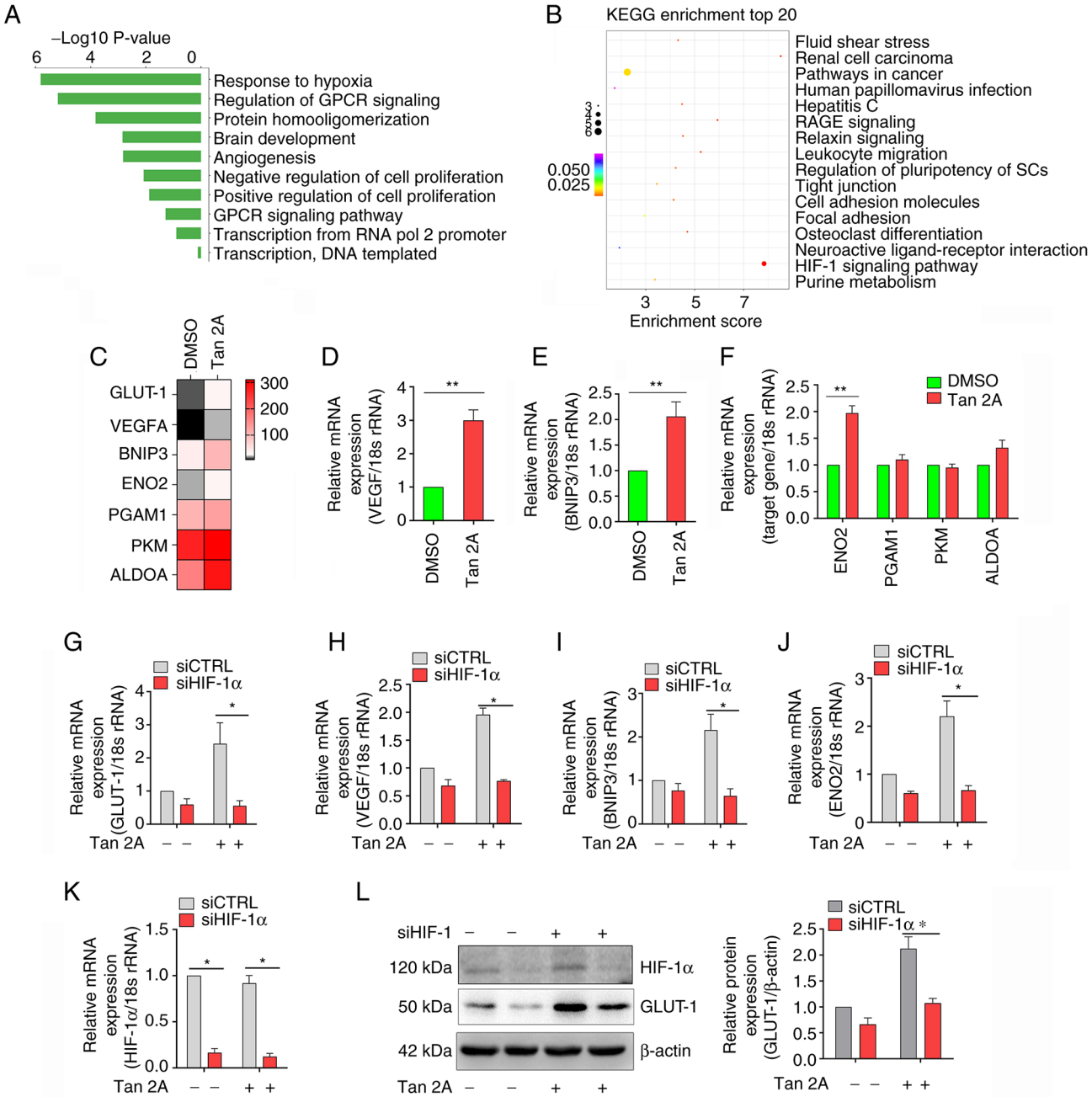

Figure 2. Effect of Tan 2A on transcriptional activity of HIF-1α in HUVECs. (A) Gene Ontology analysis of genes upregulated in Tan 2A-treated compared with control cells. (B) KEGG pathway enrichment analysis of DEGs. Color, P-value of differential gene enrichment; size of the circle, enrichment score. (C) RNA sequencing heat map for HIF-1α target genes. Color, relative expression of protein-coding genes from high (red) to low (gray). mRNA expression levels of (D) VEGF, (E) BNIP3 and (F) ENO2, PGAM1, PKM and ALDOA in control and Tan 2A-treated HUVECs analyzed using RT-qPCR (n=3). The mRNA expression levels of (G) GLUT-1, (H) VEGF, (I) BNIP3, (J) ENO2 and (K) HIF-1α in control or HIF-1α-silenced HUVECs treated with Tan 2A for 24 h were analyzed using RT-qPCR (n=3). (L) HIF-1α silenced HUVECs were treated with Tan 2A for 24 h before western blotting of GLUT-1. Data from 3 independent experiments are presented. *P<0.05 and **P<0.01. Tan 2A, Tanshinone 2A; HUVEC, human umbilical vein endothelial cell; RT-q, reverse transcription-quantitative; GLUT-1, glucose transporter 1; KEGG, Kyoto Encyclopedia of Genes and Genomes; VEGF, vascular endothelial cell growth factor; BNIP3, BCL2 interacting protein 3; ENO2, enolase 2; HIF-1α, hypoxia-inducible factor-1α; PGAM1, phosphoglycerate mutase 1; PKM, pyruvate kinase M1/2; ALDOA, aldolase; CTRL, control; si, small interfering; G Protein-Coupled Receptor, GPCR, RAGE, Receptor for AGE; stem cell (SC).

analog 2-DG. Glucose uptake in HUVECs was significantly enhanced by Tan 2A compared with DMSO control (Fig. 1E). siRNA mediated knockdown of GLUT-1 was evaluated using RT-qPCR and western blotting (Fig. 1F, G), there was a significant decrease compared with the scrambled siRNA. GLUT-1 knockdown significantly decreased the promotive effect of Tan 2A on glucose uptake compared to the scrambled siRNA control (Fig. 1H). These result demonstrated that Tan 2A induced expression of GLUT-1 and thus promoted glucose uptake in HUVECs.

Tan 2A induces expression of GLUT-1 via HIF-1α in HUVECs. RNAseq was used to evaluate the potential mechanisms of the aforementioned effect of Tan 2A in HUVECs. Gene Ontology analysis demonstrated that 'response to hypoxia' was markedly induced by Tan 2A (Fig. 2A). Kyoto Encyclopedia of

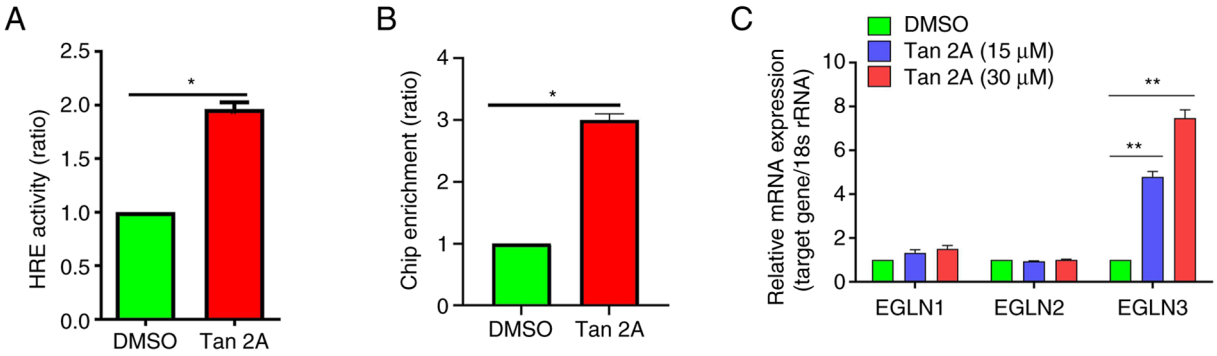

Figure 3. Tan 2A induces binding of HIF-1α to the HRE in the GLUT-1 promoter. (A) HUVECs were transfected with HRE-luc for 24 h, then treated with Tan 2A for 24 h and luciferase reporter assay was used to assess HRE activity (n=3). (B) ChIP-PCR analysis of the HIF-1α binding site in the GLUT-1 promoter. Fold enrichment of the HRE site was calculated (n=3). (C) HUVECs were treated with Tan 2A (0, 15 and 30 μM) for 24 h and the mRNA expression of EGLN1, EGLN2 and EGLN3 was analyzed by RT-qPCR (n=3). *P<0.05 and **P<0.01. Tan 2A, Tanshinone 2A; HIF-1α, hypoxia-inducible factor-1α; HRE, hypoxia-responsive element; GLUT-1, glucose transporter 1; HUVEC, human umbilical vein endothelial cell; luc, luciferase; ChIP, chromatin immunoprecipitation; EGLN, EGL-9 family hypoxia inducible factor; RT-q, reverse transcription-quantitative.

Genes and Genomes enrichment analysis demonstrated that genes were markedly enriched in 'HIF-1α signaling pathway' (Fig. 2B). Furthermore, RNA-seq analysis demonstrated that seven genes were differentially expressed (>1.5 fold) in 'HIF-1 signaling pathway', including GLUT-1, vascular endothelial growth factor A (VEGFA), BCL2 interacting protein 3 (BNIP3) and enolase 2 (ENO2) in HUVECs (Fig. 2C). The results of the RNAseq were evaluated using RT-qPCR. There were significant increases in mRNA expression levels of VEGF, BNIP3 and ENO2 following treatment with Tan 2A compared with the control (Fig. 2D-F). Knockdown of HIF-1α significantly inhibited Tan 2A-induced mRNA expression of GLUT-1, VEGFA, BNIP3 and ENO2 in HUVECs (Fig. 2G-K). Western blotting demonstrated that Tan 2A-induced protein expression of GLUT-1 was also significantly reversed by HIF-1α knockdown (Fig. 2L). These results suggested that Tan 2A regulated GLUT-1 expression in HUVECs via the HIF-1α signaling pathway.

Tan 2A increases HRE activity in HUVECs. To assess regulation of HIF-1α by Tan 2A in HUVECs, luciferase reporter assay was performed using constructs with the regulatory region of the HRE. The HRE displayed significantly increased luciferase activity in response to Tan 2A compared with the control (Fig. 3A). ChIP assay was performed to assess the regulatory effect of Tan 2A on the binding ability of HIF-1α to the potential HRE within the promoter region of the GLUT-1 gene and demonstrated that binding of HIF-1α to the promoter region of GLUT-1 gene was significantly enhanced by Tan 2A in HUVECs (Fig. 3B). HIF-1α is hydroxylated by prolyl hydroxylases (25). RT-qPCR demonstrated that Tan 2A significantly increased expression of EGL-9 family hypoxia inducible factor 3 (EGLN3), which belongs to prolyl hydroxylase family, compared with the control, these data suggested that EGLN3 mediated Tan 2A-induced activation of HIF-1α in HUVECs (Fig. 3C). These results showed Tan 2A induced HIF-1/HRE pathway in HUVECs.

RBPJκ mediates regulation of GLUT-1 by Tan 2A in HUVECs. RBPJκ binds with HIF-1α to regulate expression of downstream target genes, such as VEGFA (26). Whether RBPJκ mediates Tan 2A-regulated expression of GLUT-1 was therefore examined. RT-qPCR demonstrated that knockdown of RBPJκ significantly inhibited Tan 2A-induced mRNA expression of GLUT-1, BNIP3 and ENO2 in HUVECs (Fig. 4A-D). Furthermore, Tan 2A markedly decreased protein expression levels of GLUT-1, as demonstrated by western blotting (Fig. 4E). These data suggested that RBPJκ potentiated Tan 2A-induced GLUT-1 expression in HUVECs.

Tan 2A enhances the interaction between HIF-1α and RBPJκ protein. It has been reported that RBPJκ physically interacts with HIF protein (27). Whether Tan 2A regulates coupling between HIF-1 and RBPJκ was assessed. Western blotting of Co-IP samples demonstrated that HIF-1α was co-immunoprecipitated with RBPJκ, which suggested a physical interaction between the proteins. Furthermore, Tan 2A treatment markedly enhanced the physically interaction of RBPJκ with HIF-1α (Fig. 5).

Discussion

Under both normal and pathological conditions, the concentration of glucose in neurons is strictly controlled and relies on sustained blood flow and glucose transport (28). Therefore, altered expression of GLUT-1 at the blood-brain barrier affects the function of neurons. In the present study, Tan 2A regulated GLUT-1 expression and glucose uptake in HUVECs. Furthermore, Tan 2A enhanced the interaction between HIF-1α and RBPJκ and HIF-1α and RBPJκ mediated the effect of Tan 2A on mRNA and protein expression levels of GLUT-1. These results suggested that Tan 2A may facilitate recovery of brain function via upregulation of the GLUT-1 to increase glucose absorption.

The energy demand of neurons in the brain is served by glucose transported from the blood. Glucose is transported into brain cells via members of the GLUT family. GLUT-3 is primarily expressed in neurons, while GLUT-1 gene expression is limited to ECs in the healthy brain (29) and regulates glucose transport into the brain (30,31). Two subtypes of GLUT-1, a 55 kDa isoform in brain ECs and a 45 kDa isoform in adjacent astrocytes, have been reported previously (32).

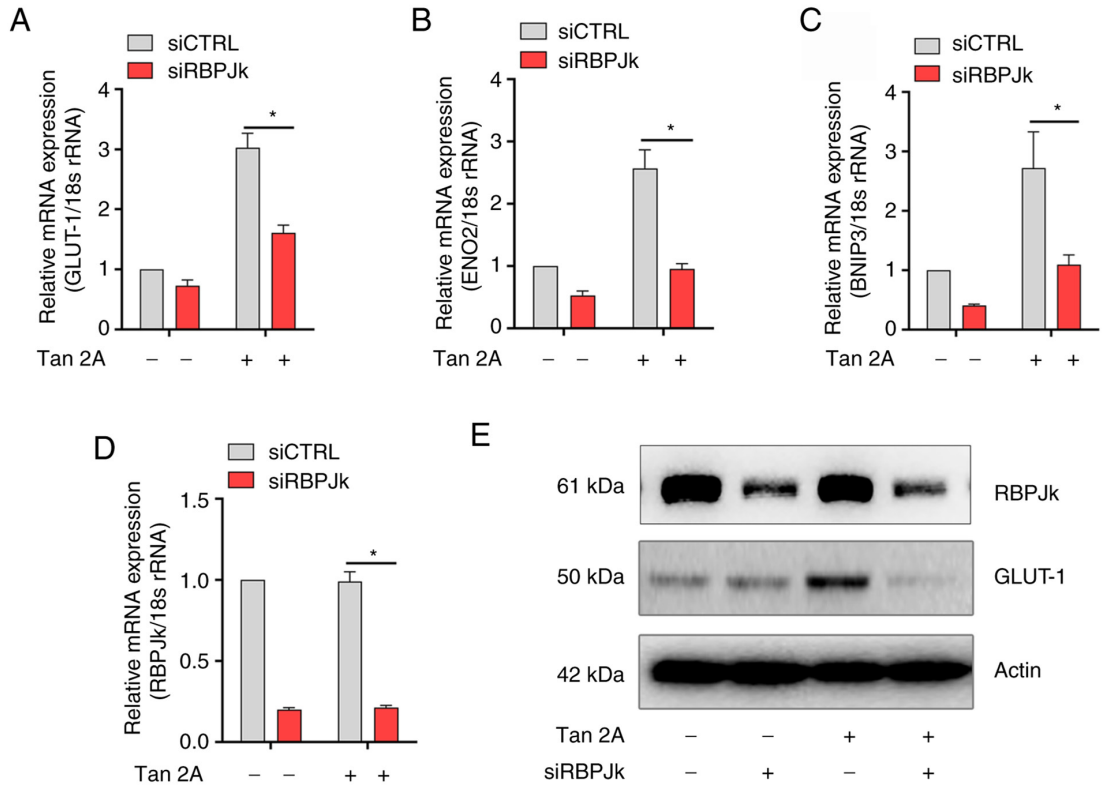

Figure 4. Knockdown of RBPJκ decreases expression of HIF-1α target genes induced by Tan 2A. RBPJκ-silenced human umbilical vein endothelial cells were stimulated with Tan 2A (15 μM) for 24 h and mRNA expression levels of (A) GLUT-1, (B) ENO2, (C) BNIP3 and (D) RBPJκ were analyzed using RT-qPCR (n=3). *P<0.05. (E) Representative western blots for GLUT-1 from 3 independent experiments. Tan 2A, Tanshinone 2A; HIF-1α, hypoxia-inducible factor-1α; RT-q, reverse transcription-quantitative; GLUT-1, glucose transporter 1; BNIP3, BCL2 interacting protein 3; ENO2, enolase 2; RBPJκ, recombination signal-binding protein for immunoglobulin κJ region; si, small interfering.

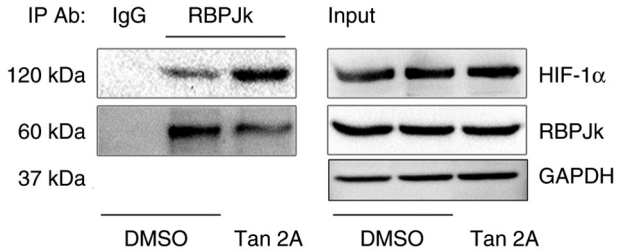

Figure 5. Tan 2A induces protein interaction between HIF-1α and RBPJκ. Human umbilical vein endothelial cells were treated with Tan 2A or DMSO for 16 h. Cellular lysate was subjected to IP with anti-RBPJκ antibodies and immunoblotted with anti-HIF-1α and anti-RBPJκ antibodies. Images are representative of three independent experiments. Tan 2A, Tanshinone 2A; HIF-1α, hypoxia-inducible factor-1α; RBPJκ, recombination signal-binding protein for immunoglobulin κJ region; IP, immunoprecipitation; Ab, antibody.

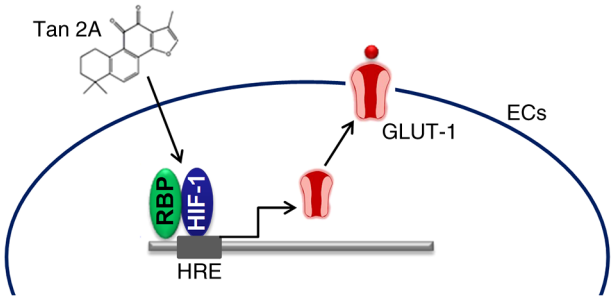

Figure 6. Schematic model of the role of Tan 2A in regulation of GLUT-1 expression. Tan 2A promotes binding of RBPJκ and HIF-1α and increased the HIF-1α induced activity of HRE to induce GLUT-1 expression in HUVECs. Tan 2A, Tanshinone 2A; HIF-1α, hypoxia-inducible factor-1α; GLUT-1, glucose transporter 1; RBP, recombination signal-binding protein; HRE, hypoxia-responsive element; EC, endothelial cell.

Previous studies have reported that changes in expression of GLUT affect the function of neurons and that GLUT-1 haploid deficiency induces decreased brain weight, activated astrocytosis, impaired motor performance and diminished brain glucose metabolism in mice (28,33). Our results showed that Tan 2A upregulated GLUT-1 expression and 2-DG uptake in HUVECs. In addition to its role in transporting glucose into the brain (34), GLUT-1 is needed for maintenance of proper brain capillary networks, blood flow and blood-brain barrier integrity (35). Furthermore, inhibition of GLUT-1 decreases EC glucose uptake and glycolysis, which leads to energy depletion, activation of the cellular energy sensor AMPK and decreased EC proliferation (5), as well as decreased nitric oxide-dependent endothelial relaxation (36).

Tan 2A is used in the treatment of cardio- and cerebrovascular disorders, such as coronary heart disease and cerebral infarction (37). Tan 2A exerts anti-atherosclerosis, anti-cardiac hypertrophy and antioxidant effects via regulation of the expression of numerous molecules, including transcription factors, scavenger receptors, ion channels, pro- and anti-apoptotic proteins, growth factors, inflammatory mediators and microRNAs (38). Tan 2A protects against cardiovascular disease via regulation of Akt/glycogen synthase

kinase-3β, nitric oxide and JNK signaling (39-41). Tan 2A treatment combined with overexpression of GLUT-1 increases glucose uptake and thus promotes viability of neurons and recovery of brain function (42). It has also been reported that treatment with Danshen and Sanqi (a kind of Chinese herbal medicine) ameliorates hyperlipidemia and hyperglycemia phenotypes in mice with diet-induced obesity via regulation of liver glycogen synthesis and cholesterol anabolism genes, including GLUT-1 (15). The present study demonstrated that Tan 2A significantly increased GLUT-1 mRNA and markedly increased GLUT-1 protein expression levels in HUVECs. Therefore, Tan 2A may serve as an adjuvant drug to treat GLUT-1-associated neuron disorder.

HIF-1 is a heterodimeric transcription factor comprising an α and β subunit. Its activity is dependent on the stability of HIF-1α. It is relatively stable under hypoxia and interacts with HIF-1β to form the HIF-1 active heterodimer (25). HIF-1α is considered to mediate cardio- and neuroprotection, partly by reprogramming cellular metabolism (43). The expression of key downstream genes, including VEGF (44), carbonic anhydrase (45) and GLUT-1 (46), is induced by HIF-1 via binding to the enhancer sequence located HRE in these genes. Our results showed that Tan 2A increased the activity of HRE of HIF-1α and the expression of VEGFA and GLUT-1. Tan 2A decreases astrocyte proliferation and significantly attenuates oxygen-glucose deprivation-induced accumulation of HIF-1α and C-X-C motif chemokine ligand 12, which blocks downstream signaling via Erk1/2 and Akt activation. By contrast with previous reports that Tan 2A inhibits transcription of HIF-1 in tumor cells, the present study demonstrated an increase in HIF-1α mRNA and protein expression levels in Tan 2A-treated HUVECs and that the binding of HIF-1α to the HRE in GLUT-1 promotor sequence was induced by Tan 2A. But how the Tan 2A activate the HIF-1α is still underdetermined. And whether Tan 2A interacts with HIF-1α or DNA sequences in target genes is not known. Previous studies have reported Tan 2A is a natural monoacylglycerol lipase (MAGL) inhibitor that interacts with the MAGL binding pocket (47). Furthermore, it has been reported that imidazole-based Tan 2A derivatives improve the selectivity and binding affinity with G-quadruplex DNA and enhances inhibition of breast cancer metastasis (48). The present study further demonstrates that HIF-1α partially mediated the regulatory effect of Tan 2A on GLUT-1 expression in ECs.

The DNA binding transcription factor RBPJκ, a key mediator of Notch signaling, recruits additional co-factors, including mastermind proteins 1-3, to activate target genes. RBPJκ is also a putative cofactor of HIF-1α (27). The association of RBPJκ with the HIF-1α complex promotes expression of replication and transcriptional activators (49). HIF-1 and HIF-2 competitively bind to the intracellular domain of the Notch receptor, an RBPJκ partner, and dynamically regulate activation of Notch signaling in glioma stem cells (50). However, RBPJκ may control gene expression of angiogenic factors by antagonizing the activity of HIF-1α (27). Deficiency of RBPJκ in mice leads to activation of HIF-1α-mediated regulation of Notch targets in hematopoietic stem and progenitor cells (51). The present study demonstrated that RBPJκ and HIF-1α knockdown both significantly reversed Tan 2A-induced mRNA expression levels of GLUT-1 and markedly decreased protein expression levels of GLUT-1 in HUVECs. Furthermore, Tan 2A markedly increased binding of HIF-1α and RBPJκ. It was therefore hypothesized that RBPJκ affects binding of HIF-1α to the HRE in the GLUT-1 promotor and that both RBPJκ and HIF-1α may be involved in regulation of GLUT-1 gene expression induced by Tan 2A. Whether Tan 2A plays the same role under anoxic conditions is still to be studied.

In summary, the present study suggested that Tan 2A induced expression of GLUT-1 via the HIF-1α signaling pathway (Fig. 6). Furthermore, Tan 2A may ameliorate brain glucose metabolism by regulating GLUT-1 mediated glucose transport in HUVECs.

Acknowledgements

Not applicable.

Funding

The present study was supported by the National Natural Science Foundation of China (grant no. 81774076) and Clinical Superior Discipline Development Fund of Shanghai Putuo District (grant no. 2019ysxk01).

Availability of data and materials

The datasets generated and/or analyzed during the current study are available in the Sequencing Read Archive repository (https://www.ncbi.nlm.nih.gov/sra/PRJNA871126).

Authors' contributions

ZL conceived and designed experiments. YZ and HZ drafted the manuscript. YZ, HZ, YH, SW and ZL performed the experiments and analyzed the data. All authors have read and approved the final manuscript. YZ and ZL confirm the authenticity of all the raw data.

Ethics approval and consent to participate

Not applicable.

Patient consent for publication

Not applicable.

Competing interests

The authors declare that they have no competing interests.

References

1. Mergenthaler P, Lindauer U, Dienel GA and Meisel A: Sugar for the brain: The role of glucose in physiological and pathological brain function. Trends Neurosci 36: 587-597, 2013.
2. Zhao FQ and Keating AF: Functional properties and genomics of glucose transporters. Curr Genomics 8: 113-128, 2007.
3. Kayano T, Fukumoto H, Eddy RL, Fan YS, Byers MG, Shows TB and Bell GI: Evidence for a family of human glucose transporter-like proteins. Sequence and gene localization of a protein expressed in fetal skeletal muscle and other tissues. J Biol Chem 263: 15245-15248, 1988.

4. Mueckler M: Facilitative glucose transporters. Eur J Biochem 219: 713-725, 1994.
5. Veys K, Fan Z, Ghobrial M, Bouche A, Garcia-Caballero M, Vriens K, Conchinha NV, Seuwen A, Schlegel F and Gorski T: Role of the GLUT1 glucose transporter in postnatal CNS angiogenesis and blood-brain barrier integrity. Circ Res 127: 466-482, 2020.
6. Nagamatsu S, Kornhauser JM, Burant CF, Seino S, Mayo KE and Bell GI: Glucose transporter expression in brain. cDNA sequence of mouse GLUT3, the brain facilitative glucose transporter isoform, and identification of sites of expression by in situ hybridization. J Biol Chem 267: 467-472, 1992.
7. Wang H, Pang W, Xu X, You B, Zhang C and Li D: Cryptotanshinone attenuates ischemia/reperfusion-induced apoptosis in myocardium by upregulating MAPK3. J Cardiovasc Pharmacol 77: 370-377, 2021.
8. Xu J, Zhang P, Chen Y, Xu Y, Luan P, Zhu Y and Zhang J: Sodium tanshinone IIA sulfonate ameliorates cerebral ischemic injury through regulation of angiogenesis. Exp Ther Med 22: 1122, 2021.
9. Subedi L and Gaire BP: Tanshinone IIA: A phytochemical as a promising drug candidate for neurodegenerative diseases. Pharmacol Res 169: 105661, 2021.
10. Zhang Y, Li C, Meng H, Guo D, Zhang Q, Lu W, Wang Q, Wang Y and Tu P: BYD ameliorates oxidative stress-induced myocardial apoptosis in heart failure post-acute myocardial infarction via the P38 MAPK-CRYAB signaling pathway. Front Physiol 9: 505, 2018.
11. Tang Q, Han R, Xiao H, Shen J, Luo Q and Li J: Neuroprotective effects of tanshinone IIA and/or tetramethylpyrazine in cerebral ischemic injury in vivo and in vitro. Brain Res 1488: 81-91, 2012.
12. Zhu J, Xu Y, Ren G, Hu X, Wang C, Yang Z, Li Z, Mao W and Lu D: Tanshinone IIA Sodium sulfonate regulates antioxidant system, inflammation, and endothelial dysfunction in atherosclerosis by downregulation of CLIC1. Eur J Pharmacol 815: 427-436, 2017.
13. Lou G, Hu W, Wu Z, Xu H, Yao H, Wang Y, Huang Q, Wang B, Wen L, Gong D, *et al*: Tanshinone II A attenuates vascular remodeling through klf4 mediated smooth muscle cell phenotypic switching. Sci Rep 10: 13858, 2020.
14. Chen W, Li X, Guo S, Song N, Wang J, Jia L and Zhu A: Tanshinone IIA harmonizes the crosstalk of autophagy and polarization in macrophages via miR-375/KLF4 pathway to attenuate atherosclerosis. Int Immunopharmacol 70: 486-497, 2019.
15. Xie Z, Truong TL, Zhang P, Xu F, Xu X and Li P: Dan-Qi prescription ameliorates insulin resistance through overall corrective regulation of glucose and fat metabolism. J Ethnopharmacol 172: 70-79, 2015.
16. Guan R, Wang J, Li Z, Ding M, Li D, Xu G, Wang T, Chen Y, Yang Q, Long Z, *et al*: Sodium tanshinone IIA sulfonate decreases cigarette smoke-induced inflammation and oxidative stress via blocking the activation of MAPK/HIF-1alpha signaling pathway. Front Pharmacol 9: 263, 2018.
17. Zhou L, Sui H, Wang T, Jia R, Zhang Z, Fu J, Feng Y, Liu N, Ji Q, Wang Y, *et al*: Tanshinone IIA reduces secretion of proangiogenic factors and inhibits angiogenesis in human colorectal cancer. Oncol Rep 43: 1159-1168, 2020.
18. Zhou ZY, Zhao WR, Xiao Y, Zhang J, Tang JY and Lee SM: Mechanism study of the protective effects of sodium tanshinone IIA sulfonate against atorvastatin-induced cerebral hemorrhage in zebrafish: Transcriptome analysis. Front Pharmacol 11: 551745, 2020.
19. Fu P, Du F, Chen W, Yao M, Lv K and Liu Y: Tanshinone IIA blocks epithelial-mesenchymal transition through HIF-1alpha downregulation, reversing hypoxia-induced chemotherapy resistance in breast cancer cell lines. Oncol Rep 31: 2561-2568, 2014.
20. Xu M, Cao F, Liu L, Zhang B, Wang Y, Dong H, Cui Y, Dong M, Xu D, Liu Y, *et al*: Tanshinone IIA-induced attenuation of lung injury in endotoxemic mice is associated with reduction of hypoxia-inducible factor 1α expression. Am J Respir Cell Mol Biol 45: 1028-1035, 2011.
21. Lu Y, Wang SJ and Song XT: Effects of electroacupuncture on glucose transporter-1 expression of hippocampal microvascular endothelial cells in rats with focal cerebral ischemia. Zhen Ci Yan Jiu 35: 118-123, 2010 (In Chinese).
22. Livak KJ and Schmittgen TD: Analysis of relative gene expression data using real-time quantitative PCR and the 2(-Delta Delta C(T)) method. Methods 25: 402-408, 2001.
23. Wang Y, Zhang Y, Zhu Y and Zhang P: Lipolytic inhibitor G0/G1 switch gene 2 inhibits reactive oxygen species production and apoptosis in endothelial cells. Am J Physiol Cell Physiol 308: C496-C504, 2015.
24. Baudin B, Bruneel A, Bosselut N and Vaubourdolle M: A protocol for isolation and culture of human umbilical vein endothelial cells. Nat Protoc 2: 481-485, 2007.
25. Masson N and Ratcliffe PJ: HIF prolyl and asparaginyl hydroxylases in the biological response to intracellular O(2) levels. J Cell Sci 116: 3041-3049, 2003.
26. Wang Y, Singh AR, Zhao Y, Du T, Huang Y, Wan X, Mukhopadhyay D, Wang Y, Wang N and Zhang P: TRIM28 regulates sprouting angiogenesis through VEGFR-DLL4-notch signaling circuit. FASEB J 34: 14710-14724, 2020.
27. Diaz-Trelles R, Scimia MC, Bushway P, Tran D, Monosov A, Monosov E, Peterson K, Rentschler S, Cabrales P, Ruiz-Lozano P and Mercola M: Notch-independent RBPJ controls angiogenesis in the adult heart. Nat Commun 7: 12088, 2016.
28. Benarroch EE: Brain glucose transporters: Implications for neurologic disease. Neurology 82: 1374-1379, 2014.
29. Szablewski L: Brain glucose transporters: Role in pathogenesis and potential targets for the treatment of Alzheimer's disease. Int J Mol Sci 22: 8142, 2021.
30. Allen A and Messier C: Plastic changes in the astrocyte GLUT1 glucose transporter and beta-tubulin microtubule protein following voluntary exercise in mice. Behav Brain Res 240: 95-102, 2013.
31. Choeiri C, Staines W, Miki T, Seino S and Messier C: Glucose transporter plasticity during memory processing. Neuroscience 130: 591-600, 2005.
32. Simpson IA, Carruthers A and Vannucci SJ: Supply and demand in cerebral energy metabolism: The role of nutrient transporters. J Cereb Blood Flow Metab 27: 1766-1791, 2007.
33. Ullner PM, Di Nardo A, Goldman JE, Schobel S, Yang H, Engelstad K, Wang D, Sahin M and Vivo DCD: Murine Glut-1 transporter haploinsufficiency: Postnatal deceleration of brain weight and reactive astrocytosis. Neurobiol Dis 36: 60-69, 2009.
34. Zlokovic BV: Neurovascular pathways to neurodegeneration in Alzheimer's disease and other disorders. Nat Rev Neurosci 12: 723-738, 2011.
35. Winkler EA, Nishida Y, Sagare AP, Rege SV, Bell RD, Perlmutter D, Sengillo JD, Hillman S, Kong P, Nelson AR, *et al*: GLUT1 reductions exacerbate Alzheimer's disease vasculo-neuronal dysfunction and degeneration. Nat Neurosci 18: 521-530, 2015.
36. Park JL, Heilig CW and Brosius FC III: GLUT1-deficient mice exhibit impaired endothelium-dependent vascular relaxation. Eur J Pharmacol 496: 213-214, 2004.
37. Gao S, Liu Z, Li H, Little PJ, Liu PA and Xu S: Cardiovascular actions and therapeutic potential of tanshinone IIA. Atherosclerosis 220: 3-10, 2012.
38. Xu S and Liu P: Tanshinone II-A: New perspectives for old remedies. Expert Opin Ther Pat 23: 149-153, 2013.
39. Sun D, Shen M, Li J, Li W, Zhang Y, Zhao L, Zhang Z, Yuan Y, Wang H and Cao F: Cardioprotective effects of tanshinone IIA pretreatment via kinin B2 receptor-Akt-GSK-3β dependent pathway in experimental diabetic cardiomyopathy. Cardiovasc Diabetol 10: 4, 2011.
40. Pan C, Lou L, Huo Y, Singh G, Chen M, Zhang D, Wu A, Zhao M, Wang S and Li J: Salvianolic acid B and tanshinone IIA attenuate myocardial ischemia injury in mice by NO production through multiple pathways. Ther Adv Cardiovasc Dis 5: 99-111, 2011.
41. Yang R, Liu A, Ma X, Li L, Su D and Liu J: Sodium tanshinone IIA sulfonate protects cardiomyocytes against oxidative stress-mediated apoptosis through inhibiting JNK activation. J Cardiovasc Pharmacol 51: 396-401, 2008.
42. Wang J, Tong H, Wang X, Wang X and Wang Y: Tanshinone IIA alleviates the damage of neurocytes by targeting GLUT1 in ischaemia reperfusion model (in vivo and in vitro experiments). Folia Neuropathol 58: 176-193, 2020.
43. Nanayakkara G, Alasmari A, Mouli S, Eldoumani H, Quindry J, McGinnis G, Fu X, Berlin A, Peters B, Zhong J and Amin R: Cardioprotective HIF-1alpha-frataxin signaling against ischemia-reperfusion injury. Am J Physiol Heart Circ Physiol 309: H867-H879, 2015.
44. Ahn GO, Seita J, Hong BJ, Kim YE, Bok S, Lee CJ, Kim KS, Lee JC, Leeper NJ, Cooke JP, *et al*: Transcriptional activation of hypoxia-inducible factor-1 (HIF-1) in myeloid cells promotes angiogenesis through VEGF and S100A8. Proc Natl Acad Sci USA 111: 2698-2703, 2014.
45. Chiche J, Ilc K, Laferriere J, Trottier E, Dayan F, Mazure NM, Brahimi-Horn MC and Pouysségur J: Hypoxia-inducible carbonic anhydrase IX and XII promote tumor cell growth by counteracting acidosis through the regulation of the intracellular pH. Cancer Res 69: 358-368, 2009.

46. Dungwa JV, Hunt LP and Ramani P: Overexpression of carbonic anhydrase and HIF-1α in wilms tumours. BMC Cancer 11: 390, 2011.
47. Yang R, Lu Y and Liu J: Identification of tanshinone IIA as a natural monoacylglycerol lipase inhibitor by combined in silico and in vitro approach. MedChemComm 5: 1528-1532, 2014.
48. Zeng L, Wu Q, Wang T, Li LP, Zhao X, Chen K, Qian J, Yuan L, Xu H and Mei WJ: Selective stabilization of multiple promoter G-quadruplex DNA by using 2-phenyl-1H-imidazole-based tanshinone IIA derivatives and their potential suppressing function in the metastatic breast cancer. Bioorg Chem 106: 104433, 2021.
49. Zhang L, Zhu C, Guo Y, Wei F, Lu J, Qin J, Banerjee S, Wang J, Shang H, Verma SC, *et al*: Inhibition of KAP1 enhances hypoxia-induced Kaposi's sarcoma-associated herpesvirus reactivation through RBP-Jκ. J Virol 88: 6873-6884, 2014.
50. Hu YY, Fu LA, Li SZ, Chen Y, Li JC, Han J, Liang L, Li L, Ji CC, Zheng MH and Hdan H: Hif-1alpha and Hif-2alpha differentially regulate Notch signaling through competitive interaction with the intracellular domain of Notch receptors in glioma stem cells. Cancer Lett 349: 67-76, 2014.
51. Lakhan R and Rathinam CV: Deficiency of Rbpj leads to defective stress-induced hematopoietic stem cell functions and hif mediated activation of non-canonical notch signaling pathways. Front Cell Dev Biol 8: 622190, 2020.